# Communication

## Ultra-Fast Perpendicular Spin–Orbit Torque MRAM

Murat Cubukcu[1], Olivier Boulle[1], Nikolaï Mikuszeit[1], Claire Hamelin[1], Thomas Brächer[1], Nathalie Lamard[2], Marie-Claire Cyrille[2], Liliana Buda-Prejbeanu[1], Kevin Garello[3], Ioan Mihai Miron[1], O. Klein[1], G. de Loubens[4], V. V. Naletov[1,4,5], Juergen Langer[6], Berthold Ocker[6], Pietro Gambardella[3], and Gilles Gaudin[1]

[1]Univ. Grenoble Alpes, CNRS, CEA, Grenoble INP, INAC-Spintec, 38000 Grenoble, France
[2]CEA Leti, F-38000 Grenoble, France
[3]Department of Materials, ETH Zurich, CH-8093 Zürich, Switzerland
[4]SPEC, CEA-Saclay, CNRS, Université Paris-Saclay, 91191 Gif-sur-Yvette, France
[5]Institute of Physics, Kazan Federal University, Kazan 420008, Russia
[6]Singulus Technologies, 63796 Kahl am Main, Germany

**We demonstrate ultra-fast (down to 400 ps) bipolar magnetization switching of a three-terminal perpendicular Ta/FeCoB/MgO/FeCoB magnetic tunnel junction. The critical current density rises significantly as the current pulse shortens below 10 ns, which translates into a minimum in the write energy in the nanosecond range. Our results show that spin–orbit torque-MRAM allows for fast and low-power write operations, which makes it promising for non-volatile cache memory applications.**

***Index Terms*— Cache memory, MRAM, spin-orbit torque-MRAM (SOT-MRAM), spin transfer, spin-orbit torque, spintronics, spin transfer torque-magnetic random access memory (STT-MRAM).**

### I. Introduction

THE introduction of non-volatility at the cache level is a major challenge to the IT industry as it would lead to a large decrease of the power consumption of microprocessors by minimizing their static- and dynamic-power consumption and pave the way toward normally OFF/instant-ON computing. Among other technologies, spin transfer torque - magnetic random access memory (STT-MRAM) has been identified as a promising candidate for the non-volatile replacement of static random access memory (SRAM) cache memory technology [1]. STT-MRAM combines CMOS compatibility, high retention time (over ten years), large endurance, and relatively fast write time (down to 4 ns for reliable switching in perpendicular STT-MRAM [2]). However, cache memory applications typically require faster operations (∼ns for L1 cache) combined with a large endurance due to their high access rate. Very fast switching (sub-ns) has been recently demonstrated using stacks where the magnetizations of the free and the fixed layers are perpendicular to the film plane [3]–[5]. However, this gain in operation speed comes at the expense of a rise in the current flowing through the tunnel barrier. As a consequence, manufacturers are currently facing reliability issues due to the accelerated aging of the tunnel barrier when injecting these high write current densities [6], [7]. Another drawback of STT-MRAM is that reading and writing use the same current path. This results in an undesired writing during the readout of the bit [7] as well as a high read power since the tunnel barrier needs to have a very small resistance to sustain the large writing current densities.

Recently, we have proposed a novel memory concept, named spin–orbit torque-MRAM (SOT-MRAM) that combines the STT advantages and naturally solves the above mentioned issues [8]–[10]. The memory is based on the discovery that a current flowing in the plane of a magnetic multilayer with structural inversion asymmetry, such as Pt/Co/$AlO_x$, exerts a torque on the magnetization, which can lead to magnetization reversal [9], [11], [12]. Such a torque arises from the conversion of the orbital to spin angular momentum through the spin Hall effect in the heavy metal and/or the Rashba–Edelstein effect at the interfaces [9], [13]–[15]. The key advantage of the SOT-MRAM is that writing and reading are decoupled due to their independent current paths. Thus, the SOT-MRAM intrinsically solves the reliability issues in current STT-MRAM promising a potentially unlimited endurance.

To be a strong candidate for non-volatile cache memory applications, SOT-MRAM needs to be fast. We recently demonstrated deterministic switching induced by current pulses shorter than 200 ps in dots made of Pt/Co/AlOx stacks [12]. However, the use of a Pt seed layer in MgO-based magnetic tunnel junction (MTJ) does not allow to reach the high tunneling magnetoresistance (TMR) ratio needed for memory applications [16], [17] (>100%), as it promotes a (111) fcc texture while a (100) bcc structure at the CoFe/MgO interface is needed to achieve high TMR [18]–[20]. On the contrary, the Ta/FeCoB/MgO/FeCoB MTJ stacks commonly used for STT-MRAM seem ideal for SOT-MRAM since they combine a high TMR, a perpendicular magnetization [21] and a large spin Hall effect in Ta [22]. In this communication, we demonstrate that magnetization

Manuscript received June 14, 2017; revised August 31, 2017; accepted October 26, 2017. Date of publication February 13, 2018; date of current version March 16, 2018. Corresponding author: O. Boulle (e-mail: Olivier.boulle@cea.fr).

Color versions of one or more of the figures in this paper are available online at http://ieeexplore.ieee.org.

Digital Object Identifier 10.1109/TMAG.2017.2772185

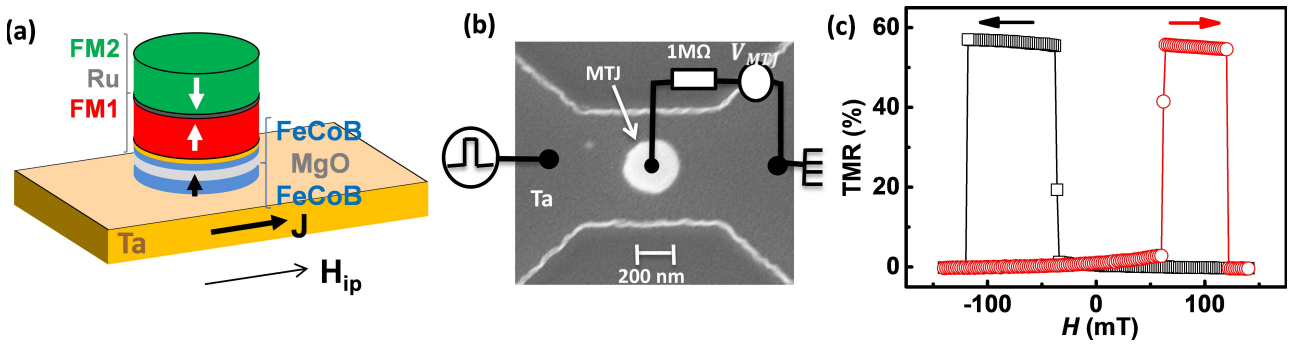


Fig. 1. (a) Sketch of the three-terminal MTJ. (b) Scanning electron microscopy image of a 275 nm diameter MTJ on top of a 635 nm wide Ta track. (c) Resistance as a function of the magnetic field applied perpendicularly to the sample plane.

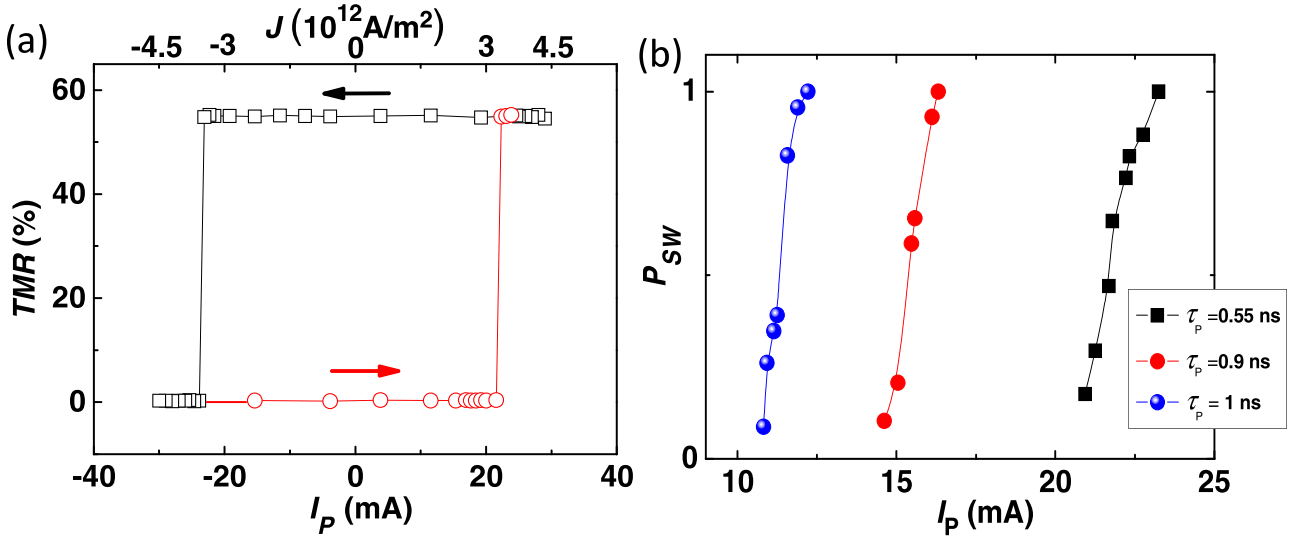


Fig. 2. (a) TMR as a function of the current pulse amplitude $I_P$ ($\tau_P = 0.55$ ns long) in the presence of an external in-plane magnetic field $\mu_0 H_{\rm ip} = 100$ mT. The TMR is measured after the injection of the current pulse. The arrows show the sweep direction of $I_P$. (b) Switching probability ($P_{\rm sw}$) from the P to the AP configuration as a function of $I_P$ for three different pulse lengths $\tau_P = 0.55$ ns (black square), $\tau_P = 0.89$ ns (red, circles) and $\tau_P = 1$ ns (blue circles) at an applied field $\mu_0 H_{\rm ip} = 100$ mT.

switching can be achieved by very short current pulses (down to 400 ps) in Ta/FeCoB/MgO three-terminal SOT-MRAM memory cells. Our results show that SOT-MRAM allows for fast and low-power write operations, rendering it promising for non-volatile cache memory applications.

## II. Experiments

The MTJs were deposited by magnetron sputtering using a SINGULUS TIMARIS deposition machine with the following structure [23]–[25] 10 Ta/1 $Fe_{60}Co_{20}B_{20}$/MgO/1.3 $Fe_{60}Co_{20}B_{20}$/0.3 Ta/$FM_1$/Ru0.85/$FM_2$ (thicknesses in nm), where $FM_1$ = [0.4 Co/ 0.4 Cu/ 1.4 Pt]$_{x5}$/0.6 Co and $FM_2$ = 0.6 Co/[0.4 Cu/ 1.4 Pt/ 0.4 Co]$_{x12}$/0.4 Cu/2 Pt [see Fig. 1(a)]. Functional three-terminal single cells with lateral dimensions down to 150 nm diameter on top of a 330 nm wide Ta track were fabricated as described in [26]. The results presented here are obtained from a sample with a 275 nm diameter MTJ on top of a 635 nm Ta track [see Fig. 1(b)]. All measurements are carried out at room temperature. Fig. 1(c) shows a typical TMR hysteresis cycle corresponding to the successive reversal of the FeCoB (1 nm) free layer and pinned layer, the magnetic field being applied perpendicularly to the sample plane. A TMR of up to 55%, associated with a sharp reversal of the magnetization of the free layer, is observed. The resistance area product of the junction is about 600 $\Omega \cdot \mu$m$^2$. For the current-induced magnetization switching experiments, current pulses are injected in the Ta bottom track using a fast voltage pulse generator whereas the TMR signal is measured using a dc voltage source connected to the MTJ in series with a 1 MΩ resistor. This resistor prevents high voltage spikes on the MTJ during the pulse injection. A 100 Ω resistor was connected in parallel to the track to minimize the impedance mismatch. The pulse rise time is 220 ps for pulse widths $\tau_P < 2$ ns, and 1.5 ns for wider pulses. The pulse width is defined as the full-width at half-maximum.

Fig. 2(a) shows the TMR signal measured after the pulse injection as a function of the amplitude of the current pulse injected in the track. An in-plane magnetic field $\mu_0 H_{\rm ip} = 100$ mT is applied along the current direction to allow for the bipolar switching [9]. The current pulse is 550 ps long. Starting from the low-resistance state and increasing the current, a sharp increase in the TMR signal is observed above a positive threshold pulse amplitude, demonstrating the reversal of the magnetization of the FeCoB bottom free layer from the parallel (P) to the anti-parallel (AP) configurations of the magnetizations. From the AP configuration, a large enough negative current allows to go back to the P configuration. This demonstrates the writing of a perpendicular SOT-MRAM

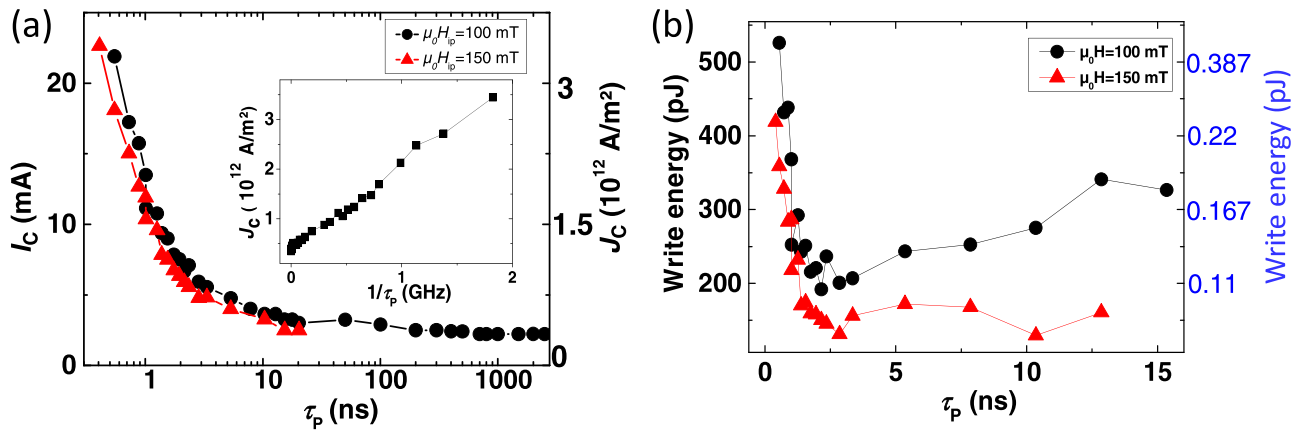


Fig. 3. (a) Switching current $I_c$ as a function of the current pulse length $\tau_P$ for two values of the external in-plane magnetic field (P to AP switching). Inset: $I_c$ versus $1/\tau_P$ for $\mu_0 H_{\rm ip} = 100$ mT. (b) Energy dissipated in a 3 kΩ resistor (simulating the resistance of the Ta track and the transistor) as a function of $\tau_P$ for two values of $H_{\rm IP}$ (three-terminal device with a 635 nm wide Ta track.) The blue scale on the right shows the write energy extrapolated for a 50 nm wide and 3 nm thick Ta track.

memory cell by a 550 ps current pulse and its reading by the TMR signal. Note that the switching current for the P to AP switching is slightly lower than the one for the AP to P, which can be explained by the dipolar interaction between the bottom free layer and the not fully compensated synthetic anti-ferromagnet. The corresponding switching current density is about $3.3 \times 10^{12}$A/m$^2$. The switching probability from the P to the AP configurations as a function of the amplitude of the current for different pulse widths is plotted in Fig. 2(b) (each point is an average over 30 events).[1] Interestingly, recent time-resolved X-ray microscopy imaging of the SOT driven magnetization reversal of Pt/Co/AlOx dots revealed that the switching probability measured electrically is not the probability of an on/off event, but more likely the fraction of the magnetic layer area that has switched [28]. These measurements show that there are no ringing or after—pulse effects associated with switching.

Magnetization switching is observed in the whole range of pulse widths from 400 ps to 2.5 $\mu$s and is bipolar: positive currents lead to a magnetization switching from P to AP, whereas negative currents lead to a switching from AP to P. The switching current $I_c$ strongly depends on the pulse length $\tau_P$ [see Fig. 3(a)]. For $\tau_P > 10$ ns, $J_c$ changes little with $\tau_P$ and scales approximately linearly on log ($\tau_P$), which suggests a thermally activated regime where stochastic fluctuations help the magnetization to overcome the reversal energy barrier [28], [29]. For $\tau_P < 10$ ns, a large increase of $J_c$ is observed as $\tau_P$ decreases and $J_c$ scales linearly on $1/\tau_P$ [see Fig. 3(a) inset]. For $\tau_P < 10$ ns, a large increase of $J_c$ is observed as $\tau_P$ decreases and $J_c$ scales linearly on $1/\tau_P$ [see Fig. 3(a) inset]. This scaling is reminiscent of early spin-transfer torque predictions [30] and experiments [31] where the injected spin current polarization is aligned along the uniaxial anisotropy axis. It is expected from the conservation of spin angular momentum, assuming the magnetization is spatially homogeneous (macrospin approximation). A different scaling is, however, expected in our SOT geometry where the current spin polarization is aligned perpendicularly to the uniaxial anisotropy axis [12], [32]. On the other hand, several experimental studies have shown that for lateral sizes typically larger than 50 nm, the magnetization reversal by spin-transfer torque and SOT occurs by domain nucleation followed by domain wall propagation [28], [33]–[40]. In such a case, a $1/\tau_P$ scaling of the critical current is expected, which expresses that the switching time is the time for a nucleated domain wall to travel across the dot.

As expected, the switching current depends also on the external in-plane magnetic field $H_{\rm ip}$ and decreases as $H_{\rm ip}$ increases [Fig. 3(a)]. The corresponding write energy $E = RI^2\tau_P$ is plotted in Fig. 3(b) as function of $\tau_P$, assuming it is dissipated in a 3 kΩ resistance standing for the Ta track and the addressing transistor. The energy depends non-monotonously on $\tau_P$ with a large increase of the energy as $\tau_P$ decreases for $\tau_P < 1$ ns. Interestingly, a minimum in the write energy is observed between 1 and 3 ns. This feature is explained by the crossover between the thermally activated regime for large pulse width and the short pulse width regime. The energy scale extrapolated for a 50 nm wide and 3 nm thick Ta track is shown in blue on the right vertical axis A write energy of about 95 fJ at 1.5 ns can be reached, associated with a write current of about 180 $\mu$A, which is similar to the best results obtained so far for current perpendicular STT-MRAM technology [42], [43].

## III. Conclusion

In conclusion, we demonstrated ultra-fast bipolar and deterministic writing (down to 400 ps) of perpendicular three-terminal SOT-MRAM single cells with a Ta/CoFeB/MgO/CoFeB MTJ structure. The switching current density rises significantly as the pulse shortens below 10 ns, which translates into a write energy minimum for pulse lengths in the nanosecond range.

These experimental results extrapolate to a switching current of around 180 $\mu$A at 1.5 ns for 50 nm track width. This makes SOT-MRAM promising for a power efficient non-volatile cache memory application.

## Acknowledgment

This work was supported by the European Commission through the Seventh Framework Program (spOt project) under

[1] "Higher current density/pulsewidth could not been probed due to the limited life time of the measured samples, which was related to unoptimized nanofabrication process and RF measurement design."

Grant 318144, in part by the French Agence Nationale de la Recherche through Project SOSPIN, and in part by the Swiss National Science Foundation under Grant 200020_172775. The work of V. V. Naletov was supported by programs Competitive Growth of KFU and CMIRA'Pro of the region Rhone-Alpes. The devices were fabricated at the Plateforme de Technologie Amont, Grenoble, France.

## REFERENCES

[1] *The International Technology Roadmap for Semiconductors*. [Online]. Available: http://www.itrs.net/Links/2013ITRS/2013Chapters/2013ERD.pdf

[2] G. Jan *et al.*, "Demonstration of fully functional 8 Mb perpendicular STT-MRAM chips with sub-5ns writing for non-volatile embedded memories," in *Symp. VLSI Technol. (VLSI-Technology), Dig. Tech. Papers*, Jun. 2014, pp. 1–2.

[3] H. Liu, D. Bedau, D. Backes, J. A. Katine, J. Langer, and A. D. Kent, "Ultrafast switching in magnetic tunnel junction based orthogonal spin transfer devices," *Appl. Phys. Lett.*, vol. 97, no. 24, p. 242510, 2010.

[4] M. Marins de Castro *et al.*, "Precessional spin-transfer switching in a magnetic tunnel junction with a synthetic antiferromagnetic perpendicular polarizer," *J. Appl. Phys.*, vol. 111, no. 7, pp. 07C912-1–07C912-3, Apr. 2012.

[5] G. E. Rowlands *et al.*, "Deep subnanosecond spin torque switching in magnetic tunnel junctions with combined in-plane and perpendicular polarizers," *Appl. Phys. Lett.*, vol. 98, no. 10, p. 102509, Mar. 2011.

[6] G. Panagopoulos, C. Augustine, and K. Roy, "Modeling of dielectric breakdown-induced time-dependent STT-MRAM performance degradation," in *Proc. 69th Annu. Device Res. Conf. (DRC)*, Jun. 2011, pp. 125–126.

[7] W. S. Zhao *et al.*, "Failure and reliability analysis of STT-MRAM," *Microelectron. Rel.*, vol. 52, nos. 9–10, pp. 1848–1852, Sep. 2012.

[8] G. Gaudin, I. M. Miron, P. Gambardella, and A. Schuhl, "Writable magnetic memory element," U.S. Patent 2012 0020 152 A1, Jan. 26, 2012.

[9] I. M. Miron *et al.*, "Perpendicular switching of a single ferromagnetic layer induced by in-plane current injection," *Nature*, vol. 476, no. 7359, pp. 189–193, Aug. 2011.

[10] G. Prenat, K. Jabeur, G. D. Pendina, O. Boulle, and G. Gaudin, "Beyond STT-MRAM, spin orbit torque RAM SOT-MRAM for high speed and high reliability applications," in *Spintronics-Based Computing*. W. Zhao and G. Prenat, Eds. Springer, 2015, pp. 145–157.

[11] C. O. Avci *et al.*, "Magnetization switching of an MgO/Co/Pt layer by in-plane current injection," *Appl. Phys. Lett.*, vol. 100, no. 21, p. 212404, May 2012.

[12] K. Garello *et al.*, "Ultrafast magnetization switching by spin-orbit torques," *Appl. Phys. Lett.*, vol. 105, no. 21, p. 212402, Nov. 2014.

[13] L. Liu, C.-F. Pai, Y. Li, H. W. Tseng, D. C. Ralph, and R. A. Buhrman, "Spin-torque switching with the giant spin Hall effect of tantalum," *Science*, vol. 336, no. 6081, pp. 555–558, May 2012.

[14] K. Garello *et al.*, "Symmetry and magnitude of spin-orbit torques in ferromagnetic heterostructures," *Nature Nanotechnol.*, vol. 8, pp. 587–593, Jul. 2013.

[15] J. Kim *et al.*, "Layer thickness dependence of the current-induced effective field vector in Ta|CoFeB|MgO," *Nature Mater.*, vol. 12, pp. 240–245, Dec. 2012.

[16] Y. J. Song *et al.*, "Highly functional and reliable 8 Mb STT-MRAM embedded in 28 nm logic," in *IEDM Tech. Dig.*, Dec. 2016, pp. 27.2.1–27.2.4.

[17] J. J. Kan *et al.*, "Systematic validation of 2x nm diameter perpendicular MTJ arrays and MgO barrier for sub-10 nm embedded STT-MRAM with practically unlimited endurance," in *IEDM Tech. Dig.*, Dec. 2016, pp. 27.4.1–27.4.4.

[18] S. S. P. Parkin *et al.*, "Giant tunnelling magnetoresistance at room temperature with MgO (100) tunnel barriers," *Nature Mater.*, vol. 3, pp. 862–867, Oct. 2004.

[19] W. H. Butler, X.-G. Zhang, T. C. Schulthess, and J. M. MacLaren, "Spin-dependent tunneling conductance of Fe|MgO|Fe sandwiches," *Phys. Rev. B, Condens. Matter*, vol. 63, no. 5, p. 054416, Jan. 2001.

[20] S. Yuasa, T. Nagahama, A. Fukushima, Y. Suzuki, and K. Ando, "Giant room-temperature magnetoresistance in single-crystal Fe/MgO/Fe magnetic tunnel junctions," *Nature Mater.*, vol. 3, pp. 868–871, Oct. 2004.

[21] S. Ikeda *et al.*, "A perpendicular-anisotropy CoFeB–MgO magnetic tunnel junction," *Nature Mater.*, vol. 9, no. 9, pp. 721–724, Sep. 2010.

[22] L. Liu, C.-F. Pai, Y. Li, H. W. Tseng, D. C. Ralph, and R. A. Buhrman, "Spin-torque switching with the giant spin Hall effect of tantalum," *Science*, vol. 336, no. 6081, pp. 555–558, May 2012.

[23] D. C. Worledge *et al.*, "Spin torque switching of perpendicular Ta|CoFeB|MgO-based magnetic tunnel junctions," *Appl. Phys. Lett.*, vol. 98, no. 2, p. 022501, 2011.

[24] L. Cuchet, B. Rodmacq, S. Auffret, R. C. Sousa, C. Ducruet, and B. Dieny, "Influence of a Ta spacer on the magnetic and transport properties of perpendicular magnetic tunnel junctions," *Appl. Phys. Lett.*, vol. 103, no. 5, p. 052402, 2013.

[25] L. Cuchet, B. Rodmacq, S. Auffret, R. C. Sousa, and B. Dieny, "Influence of magnetic electrodes thicknesses on the transport properties of magnetic tunnel junctions with perpendicular anisotropy," *Appl. Phys. Lett.*, vol. 105, no. 5, p. 052408, Aug. 2014.

[26] M. Cubukcu *et al.*, "Spin-orbit torque magnetization switching of a three-terminal perpendicular magnetic tunnel junction," *Appl. Phys. Lett.*, vol. 104, no. 4, p. 042406, Jan. 2014.

[27] Higher current density/pulse width could not been probed due to the limited life time of the measured samples, which was related to unoptimized nanofabrication process and RF measurement design.

[28] M. Baumgartner *et al.*, "Spatially and time-resolved magnetization dynamics driven by spin–orbit torques," *Nature Nanotechnol.*, vol. 12, pp. 980–986, Aug. 2017.

[29] K.-S. Lee, S.-W. Lee, B.-C. Min, and K.-J. Lee, "Thermally activated switching of perpendicular magnet by spin-orbit spin torque," *Appl. Phys. Lett.*, vol. 104, no. 7, p. 072413, Feb. 2014.

[30] E. B. Myers, F. J. Albert, J. C. Sankey, E. Bonet, R. A. Buhrman, and D. C. Ralph, "Thermally activated magnetic reversal induced by a spin-polarized current," *Phys. Rev. Lett.*, vol. 89, no. 19, p. 196801, Oct. 2002.

[31] J. Z. Sun, "Spin-current interaction with a monodomain magnetic body: A model study," *Phys. Rev. B, Condens. Matter*, vol. 62, no. 1, pp. 570–578, 2000.

[32] P. M. Braganca, O. Ozatay, A. G. F. Garcia, O. J. Lee, D. C. Ralph, and R. A. Buhrman, "Enhancement in spin-torque efficiency by nonuniform spin current generated within a tapered nanopillar spin valve," *Phys. Rev. B, Condens. Matter*, vol. 77, no. 14, p. 144423, Apr. 2008.

[33] J. Park, G. E. Rowlands, O. J. Lee, D. C. Ralph, and R. A. Buhrman, "Macrospin modeling of sub-ns pulse switching of perpendicularly magnetized free layer via spin-orbit torques for cryogenic memory applications," *Appl. Phys. Lett.*, vol. 105, no. 10, pp. 102404-1–102404-5, Sep. 2014.

[34] G. Yu *et al.*, "Magnetization switching through spin-Hall-effect-induced chiral domain wall propagation," *Phys. Rev. B, Condens. Matter*, vol. 89, no. 10, p. 104421, Mar. 2014.

[35] M. M. Decker *et al.*, "Time resolved measurements of the switching trajectory of Pt/Co elements induced by spin-orbit torques," *Phys. Rev. Lett.*, vol. 118, no. 25, p. 257201, Jun. 2017.

[36] D. P. Bernstein *et al.*, "Nonuniform switching of the perpendicular magnetization in a spin-torque-driven magnetic nanopillar," *Phys. Rev. B, Condens. Matter*, vol. 83, p. 180410(R), May 2011.

[37] C. Zhang, S. Fukami, H. Sato, F. Matsukura, and H. Ohno, "Spin-orbit torque induced magnetization switching in nano-scale Ta/CoFeB/MgO," *Appl. Phys. Lett.*, vol. 107, no. 1, p. 012401, Jul. 2015.

[38] H. Sato *et al.*, "Junction size effect on switching current and thermal stability in CoFeB/MgO perpendicular magnetic tunnel junctions," *Appl. Phys. Lett.*, vol. 99, no. 4, p. 042501, 2011.

[39] J. Z. Sun *et al.*, "Effect of subvolume excitation and spin-torque efficiency on magnetic switching," *Phys. Rev. B, Condens. Matter*, vol. 84, no. 6, p. 064413, Aug. 2011.

[40] C. J. Durrant, R. J. Hicken, Q. Hao, and G. Xiao, "Scanning Kerr microscopy study of current-induced switching in Ta/CoFeB/MgO films with perpendicular magnetic anisotropy," *Phys. Rev. B, Condens. Matter*, vol. 93, no. 1, p. 014414, Jan. 2016.

[41] O. J. Lee *et al.*, "Central role of domain wall depinning for perpendicular magnetization switching driven by spin torque from the spin Hall effect," *Phys. Rev. B, Condens. Matter*, vol. 89, pp. 024418-1–024418-8, Jan. 2014.

[42] D. Saida *et al.*, "Low-current high-speed spin-transfer switching in a perpendicular magnetic tunnel junction for cache memory in mobile processors," *IEEE Trans. Magn.*, vol. 50, no. 11, pp. 1–5, Nov. 2014.

[43] L. Thomas *et al.*, "Perpendicular spin transfer torque magnetic random access memories with high spin torque efficiency and thermal stability for embedded applications (invited)," *J. Appl. Phys.*, vol. 115, no. 17, pp. 172615-1–172615-6, May 2014.